

ECE5320

Lecture #5

NANO-PARTICLE FUSION REVISITED

REMEMBER:

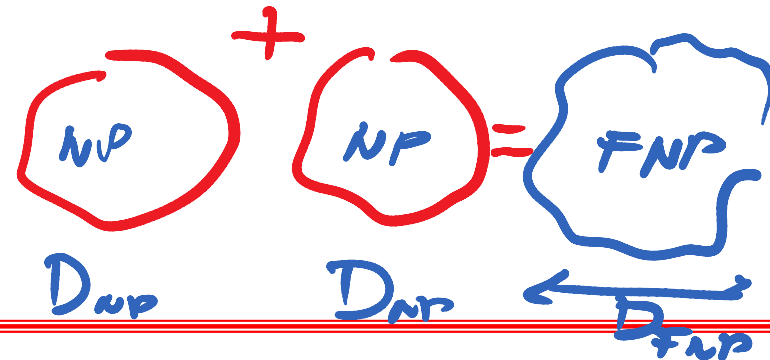
$$\Delta T_{\text{fusion}} = \frac{\Delta h_m}{S_{\text{ho}} \cdot C_p} \cdot \frac{6}{\pi D_{\text{NPF}}} \quad (1)$$

↑ FUSED NP

$$\Delta h_m = \Delta U_f = \gamma \Delta A_{\uparrow} = \gamma \pi D^2 (2 - 2^{2/3})$$

$$\Delta T_{\text{fusion}} = \frac{\gamma}{S C_p} \cdot \frac{0.413}{D_{\text{FNP}}} \quad (2)$$

AREA DECREASE



NANO-PARTICLE FUSION - REVISITED

MELTING IS POSSIBLE DURING NP FUSION

$$T_{NP} = T_{Bulk} - \Delta T(D)$$

$$T_{NP} = T_{Bulk} - \frac{6MT_{Bulk}\gamma_m}{D\Delta U_{np}g_m} \cdot \alpha \quad (2)$$

$$\alpha = \left[1 - \left(\frac{\gamma_s}{\sigma_a} \right) \cdot \left(\frac{\rho_l}{\rho_s} \right)^{2/3} \right]$$

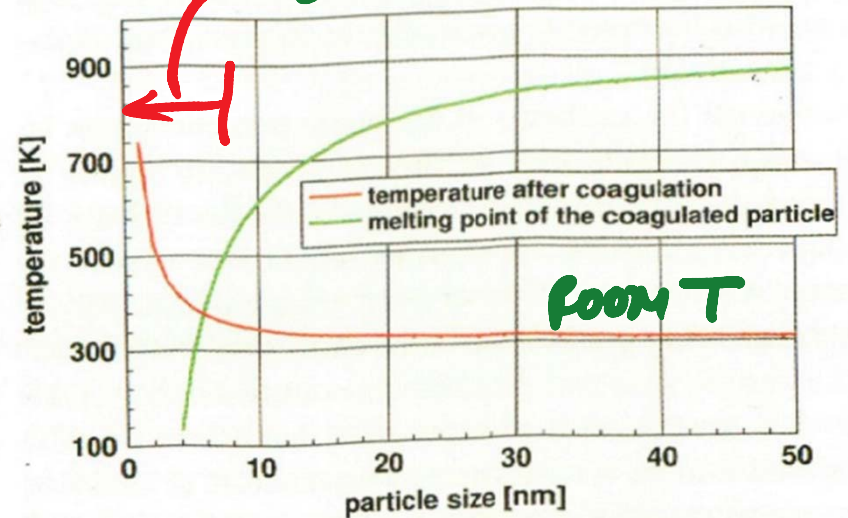


Figure 3.13 Temperature after coagulation of two aluminum particles of equal size. The melting temperature of aluminum nanoparticles is plotted as a function of particle size. Temperature flashing during coagulation may cause melting of the coagulated particle.

COMBINING (1) OR (1)' WITH 2

STRUCTURES OF NP

- Exp. OBSERVATION:
NP TAKE STRUCTURE
OF THE HIGH TEMP-
STABLE BULK PHASE

- Why: ?

- ONE REASON $T_w / pT \downarrow$

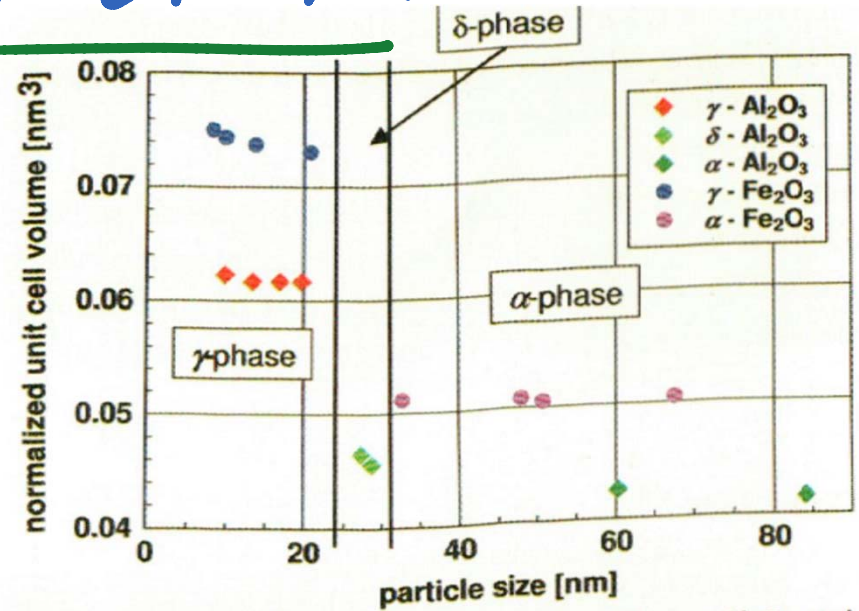
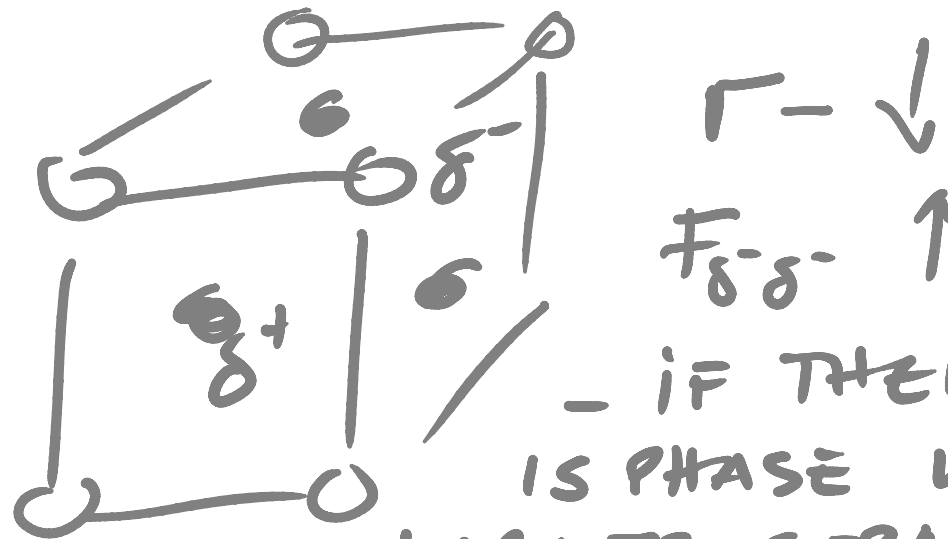
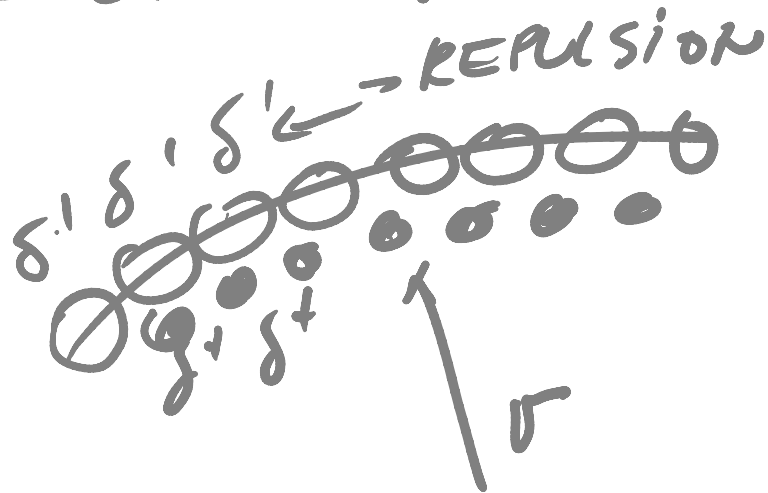


Figure 3.14 Normalized unit cell volume for different Al₂O₃ and Fe₂O₃ phases as a function of grain size [15]. Normalization provides a constant number of formula units per unit cell; otherwise, comparison is impossible. In the γ-phase, the unit cell volume is increased as the particle size decreases. A preference for high-temperature structures as the particle size decreases is clearly visible.

STRUCTURE OF NP_s

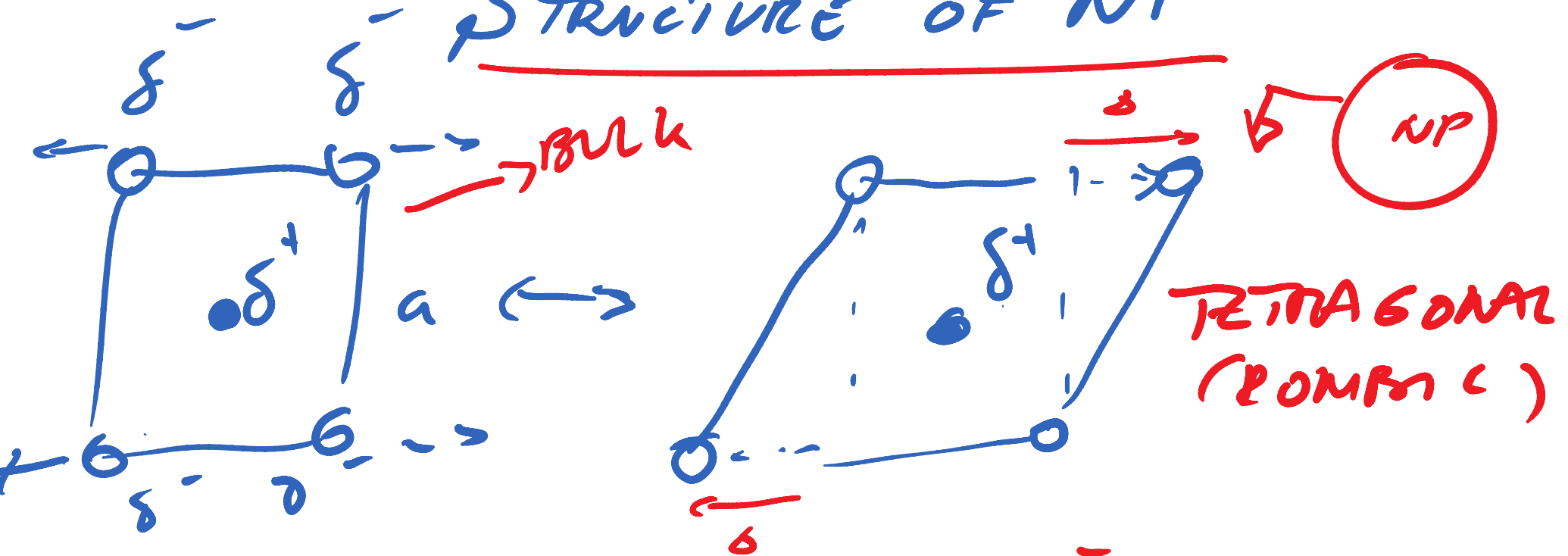
- GENERAL RULE: NP TAKE THE PHASE THAT HAS MORE SYMMETRIC ARRANGEMENT.

- OXIDES:



- IF THERE IS PHASE WITH LARGER SEPARAT. ONE IS TAKEN BY NP.

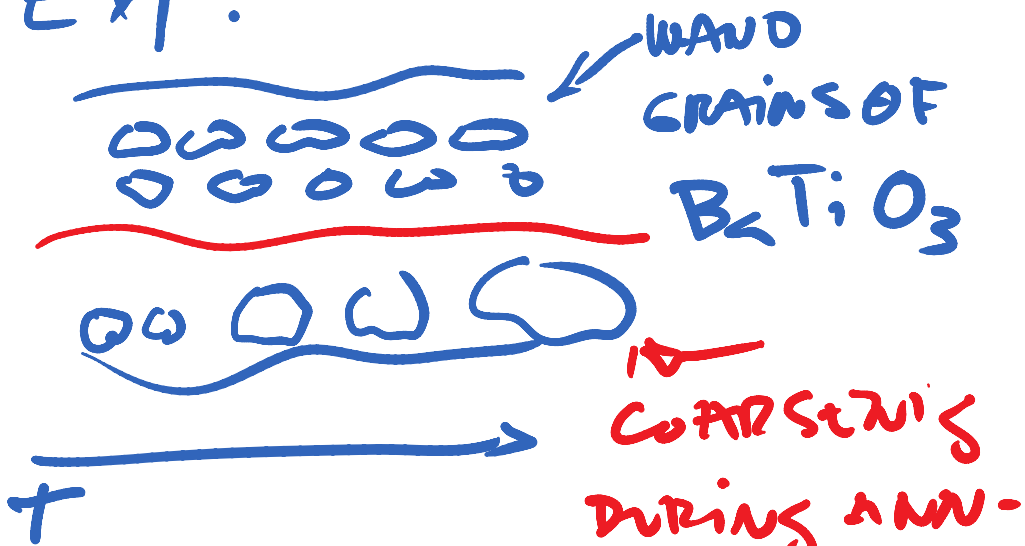
STRUCTURE OF NP



→ DUE TO OXIGEN δ^- - REPULSION PHASE THAT IS STABLE AT $\uparrow T$, IS TAKEN!

STRUCTURE OF NP

Exp:



NP / NG \rightarrow D - INCREASE

NANO GRAINS

LATTICE CONTRACTS

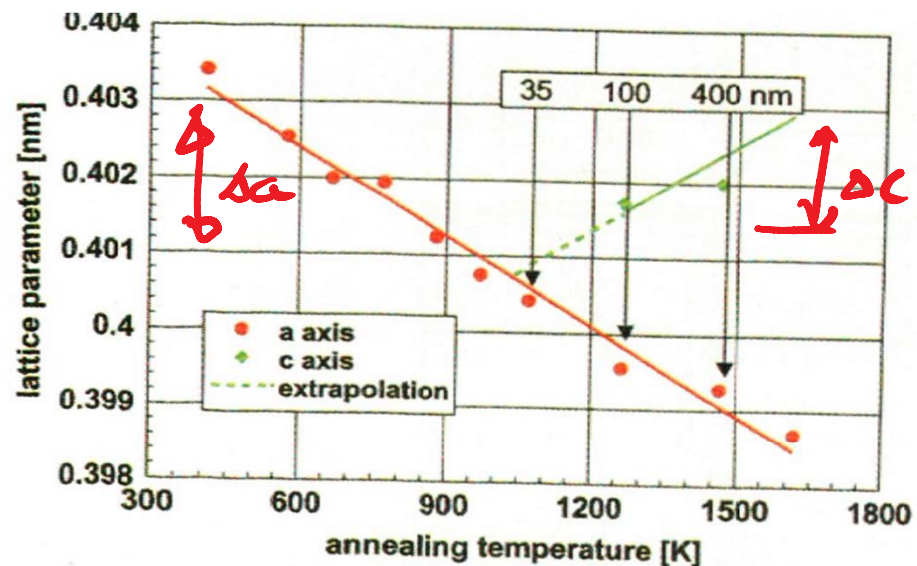


Figure 3.15 Lattice parameter of nanoparticulate $BaTiO_3$, a ferroelectric material with perovskite structure, as a function of the annealing temperature. During annealing, grain growth occurred [16]; hence, an increasing annealing temperature was equivalent to an increasing grain size. All lattice parameters were measured at room temperature, and particle sizes determined by electron microscopy. For details, see the text.

Different Exp. SAME CONCLUS.

BaTiO₃ - CUBIC STRUCTURE
 - NO DIFFERENT HIGH T STABLE STRUCTURE

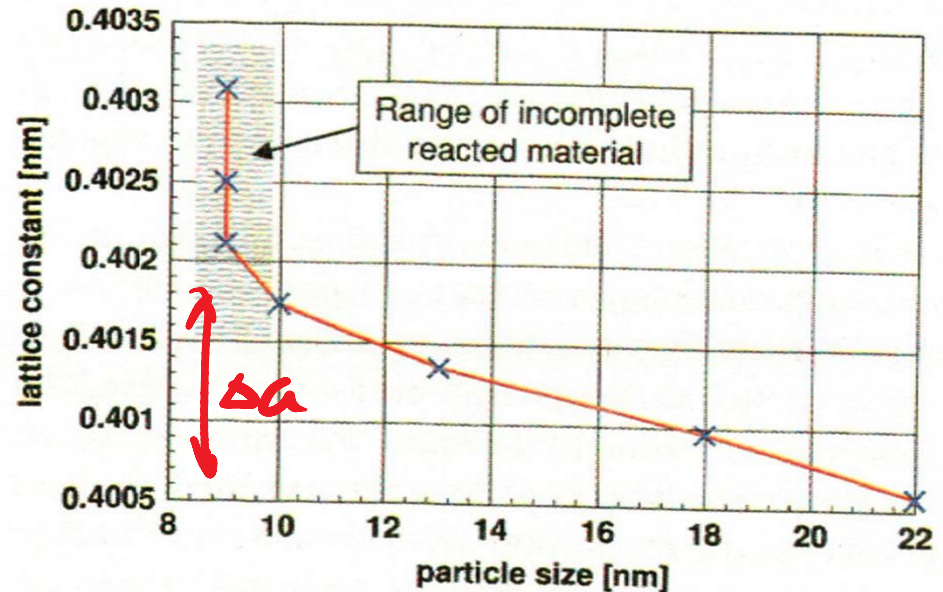
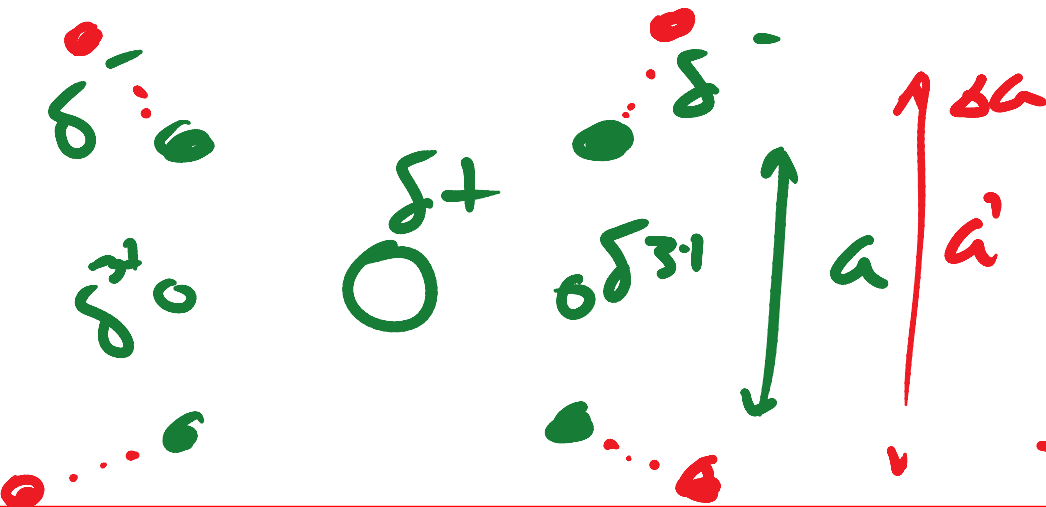


Figure 3.16 Lattice constant of BaTiO₃ in the cubic structure as a function of particle size [16]. The lattice constant decreases with increasing particle size. Values in the shaded area were deemed unreliable as the material was not completely reacted.

For $D \downarrow a \uparrow$

STRUCTURE OF NPs

- FERROELECTRIC MATERIALS
- HIGH T PHASE IS DISORDERED
- LOW T PHASE IS ORDERED

NP - DISORDERED PHASE

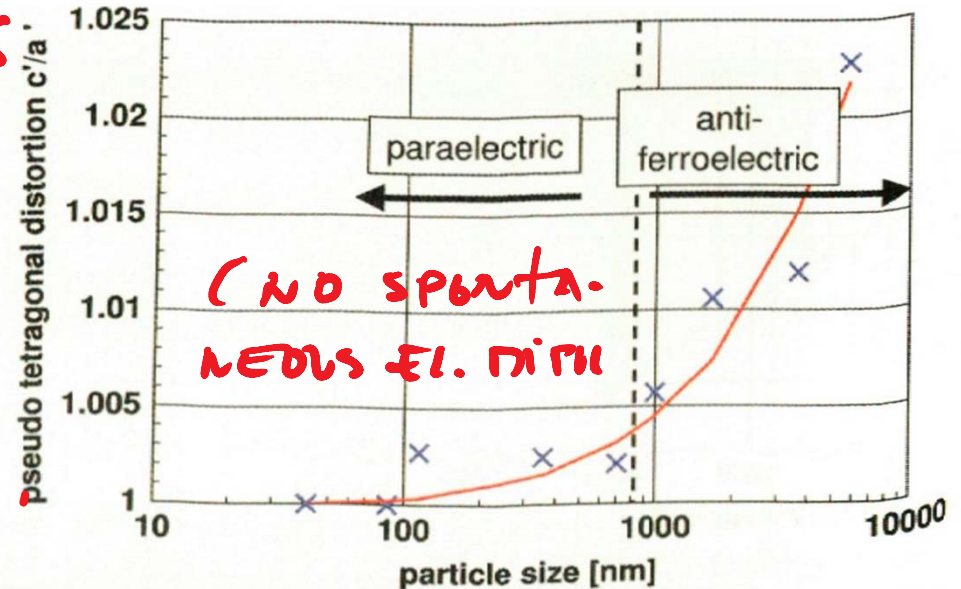


Figure 3.17 Pseudotetragonal distortion and the transition paraelectric–antiferroelectric of PbZrO_4 as a function of grain size [15]. A reduction in grain size had a similar effect as an increase in temperature. The paraelectric, cubic phase was the high-temperature phase; the antiferroelectric, tetragonal distorted phase was the low-temperature phase.

STRUCTURE OF NPs

- CURIE TEMP, T_c

ORDER DISORDER
PHASE TRANSITION T

- $V \downarrow$, $\Delta T \uparrow$, $T_c \downarrow$

- EFFECT IS THE SAME
AS INCREASING T

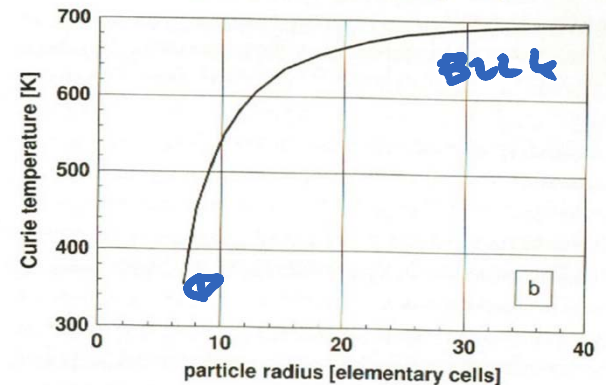
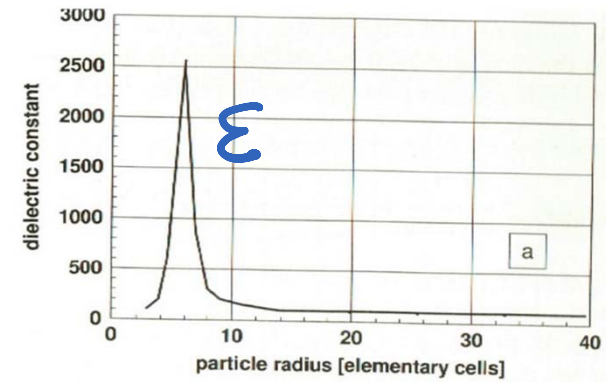


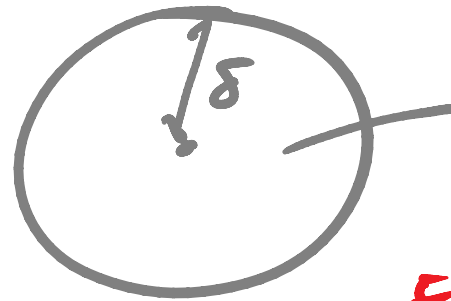
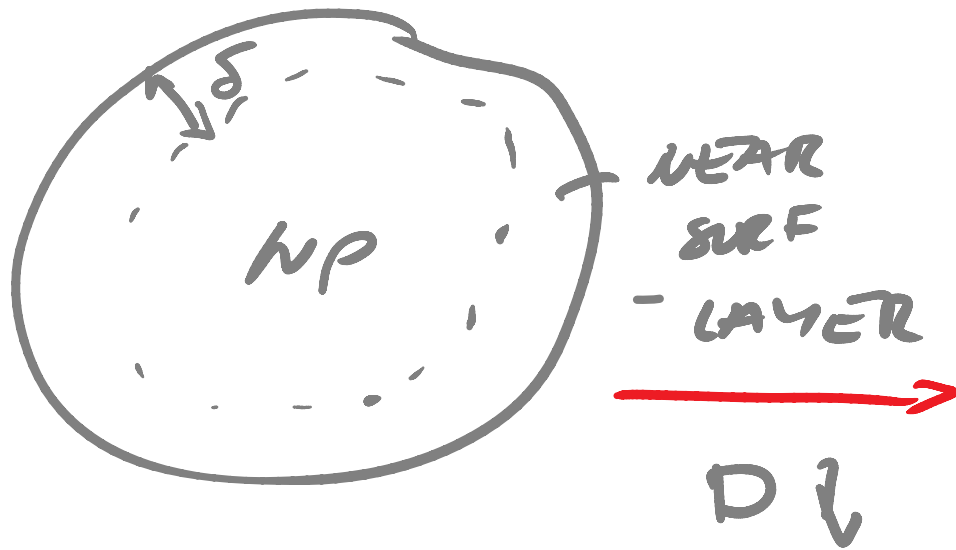
Figure 3.18 Dielectric constant and Curie temperature of $\text{PbZr}_{0.3}\text{Ti}_{0.7}\text{O}_3$ [17]. For small particle sizes transition occurs to the paraelectric, high-temperature phase. A reduction in particle size and high temperature has similar effects on particle structure and properties. The lattice constant ($a = 0.8 \text{ nm}$) was selected as the dimension for the ordinate. (a) Dielectric constant of $\text{PbZr}_{0.3}\text{Ti}_{0.7}\text{O}_3$. At small particle sizes (< 5.6 lattice constants; the material was in the paraelectric, high-temperature phase, whereas at large sizes the material was ferroelectric. (b) Curie temperature of $\text{PbZr}_{0.3}\text{Ti}_{0.7}\text{O}_3$. Below size of eight lattice constants, the T_c was no longer defined. The material was paraelectric, independent of the temperature.

LANDAU'S ORDER PARAM. M

$M = 1$ - IDEAL CRYSTAL

$M = 0$ - MELT (LIQUID)

M IS ENTROPICAL DESCRIPTION OF CRYSTAL ORDER AND DEGREES OF ATOM MOTION/FREEDOM.



VOLUME FRACTION OF THE WHOLE NP IS 1 AFFECTED BY SURF.

M FOR NP

$M \rightarrow 0$ AS

$D \rightarrow 0$

DISORDER IN NP
INCREASES AS NP
DIAMETER DECREASES
(METAL NP!)

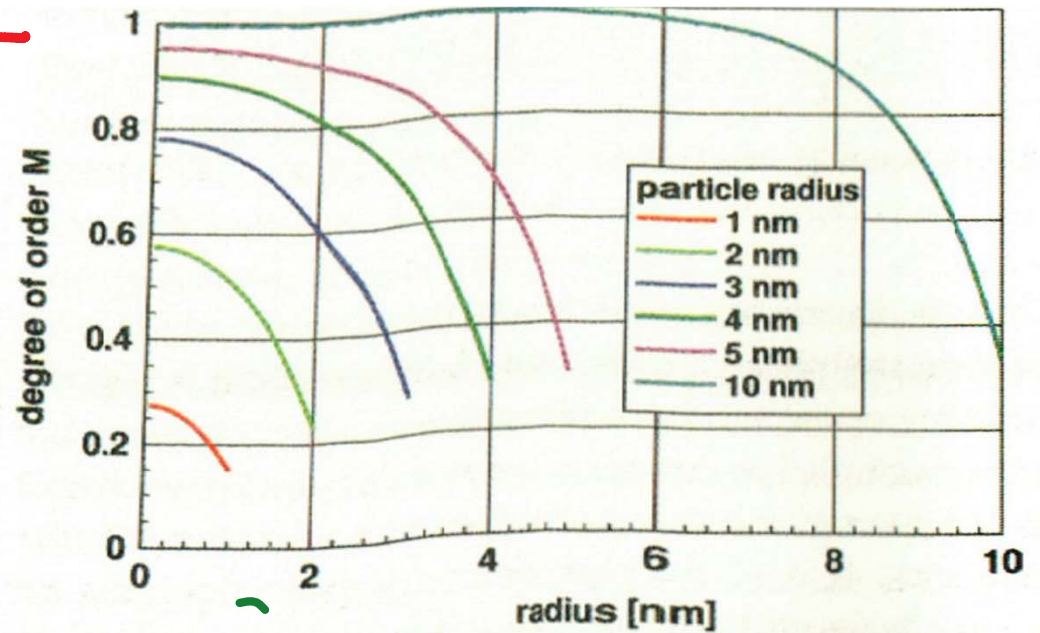
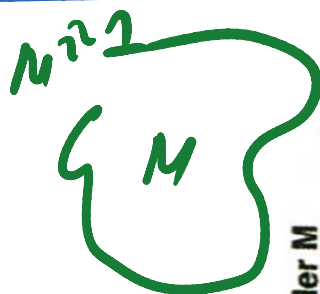


Figure 3.19 Landau's order parameter M for nanoparticles of tin as a function of radius and particle size [18]. The degree of order decreased with decreasing particle radius, and also from the interior to the surface. For perfectly crystallized particles $M = 1$; for melted particles, $M = 0$.

M FOR NP

$$M \ll 1$$



$T = \text{const.}$

$\sqrt{\uparrow}$



$M \rightarrow 1$

M - IS AN AVERAGE OF ATOMS ORDERING IN NP.

SURF. SUBORD. EFFECT. AND T_m

3.6 A Closer

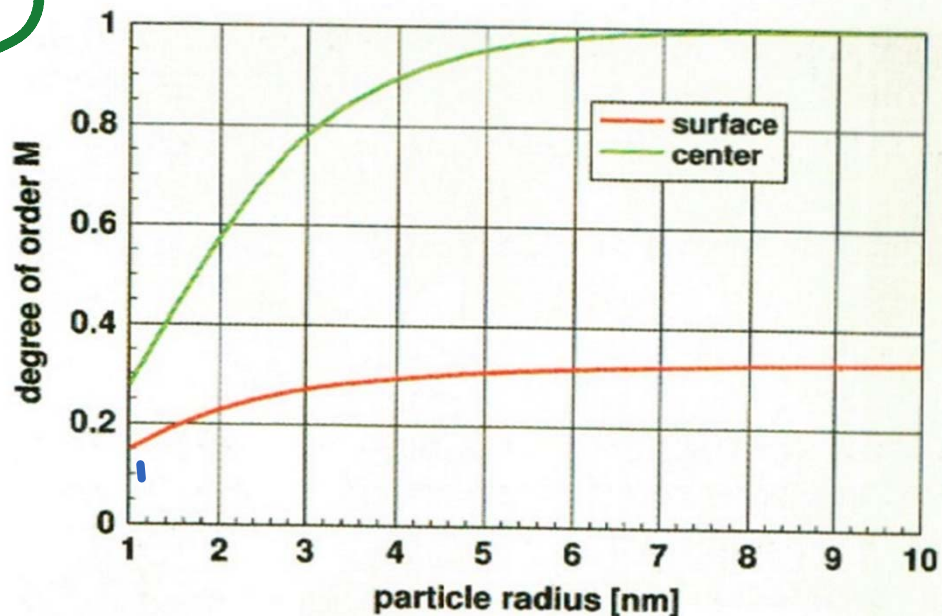


Figure 3.20 Landau's order parameter M in the center and at the surface of nanoparticles [18]. Small nanoparticles with radii < 5 nm never show perfect crystallization.

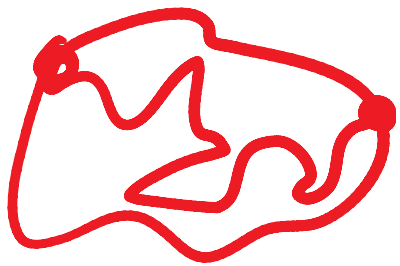
SHAPE FLUCTUATION OF NP

$$\chi^2 = D t$$

$$\downarrow \quad \downarrow$$

$$10^{-16} \text{ m}^2 \quad 10^{-12} \frac{\text{m}^2}{\text{s}}$$

$$t = 10^{-4} \text{ s}; \quad 100 \mu\text{s}$$



SURFACE
IS VERY
DYNAMIC

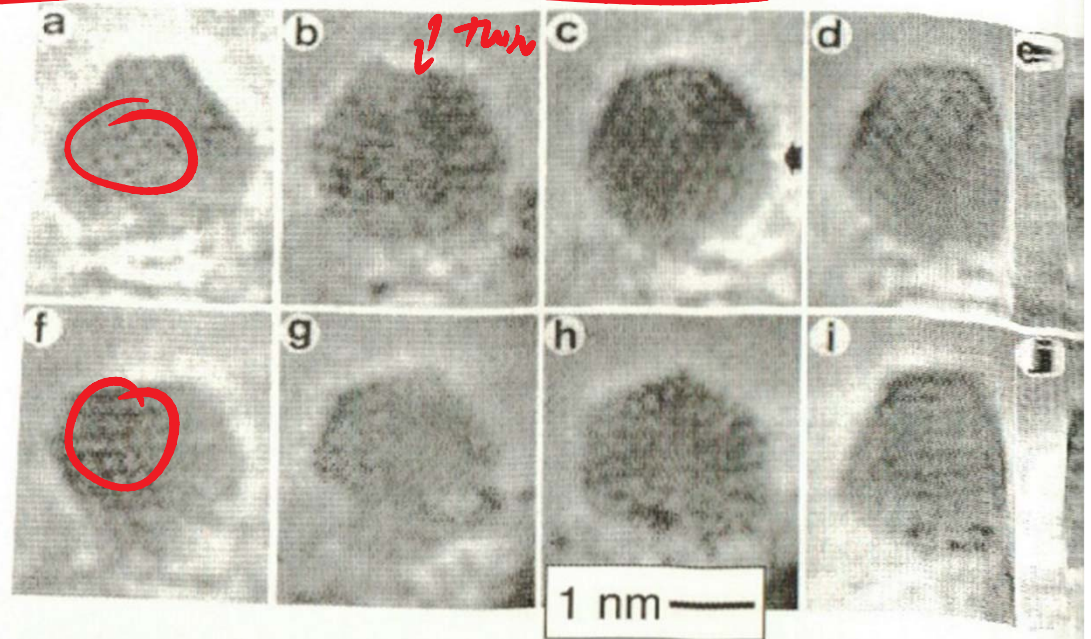


Figure 3.21 A series of electron micrographs of 2-nm gold particles [19], taken at intervals of 1/60 s. The images show spontaneous changes in particle habitus at a temperature of approximately 370 K, from single twins (a, d, and i) to multiple twinned icosahedral particles (b and h) and further to cuboctahedral shapes (e, f, and i). Copyright: American Physical Society 1986.

NP - Phase Diagram

- COMBINATION OF $T_m(V)$ AND SURF SUBORDINATION RESULTS IN STABILITY REGIMES WHICH ARE $f(V)$ FOR NP METAL!

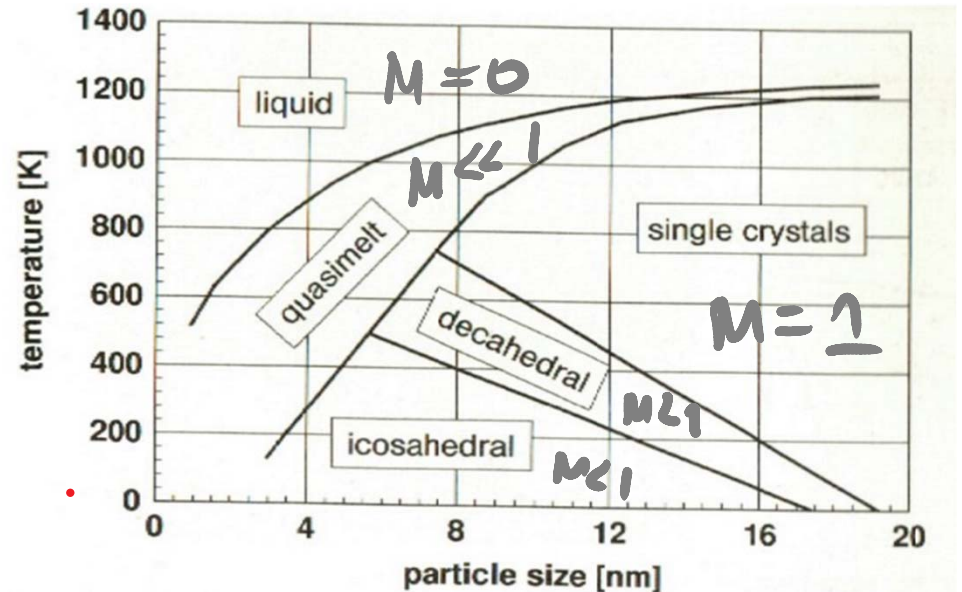


Figure 3.22 Phase diagram of gold nanoparticles, showing regions of different well-defined habitus. A region termed quasimelt is also indicated where the particles change their habitus spontaneously [20].

NP

TEM EVIDENCE

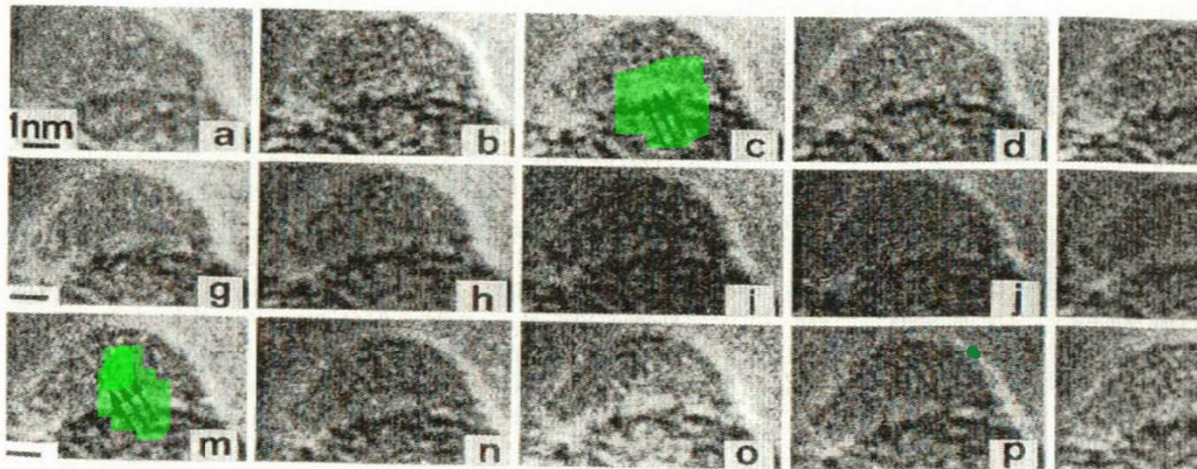


Figure 3.23 A series of electron micrographs of tin particles, taken at intervals of $1/60$ s [21]. In these images the appearance and disappearance of small crystallized regions, called embryos, can be seen within the particles (frames c and m). The phenomenon of “pseudocrystalline particles” can be attributed to a well-defined particle size–temperature range in a phase diagram (Reprinted with permission from Springer 1993.)

DIFFICULT TO OBSERVE TRA-
NSITIONS $1/60$ s PER
IMAGE:

MD SIMULATION

MD Simulations of NP dynamics

STRUCTURE OF NP

Room T:

- VERY FAST DYNAMIC,
- RESURFACING OF NP IS DONE WITHIN $\sim 10^{-3}$ s.

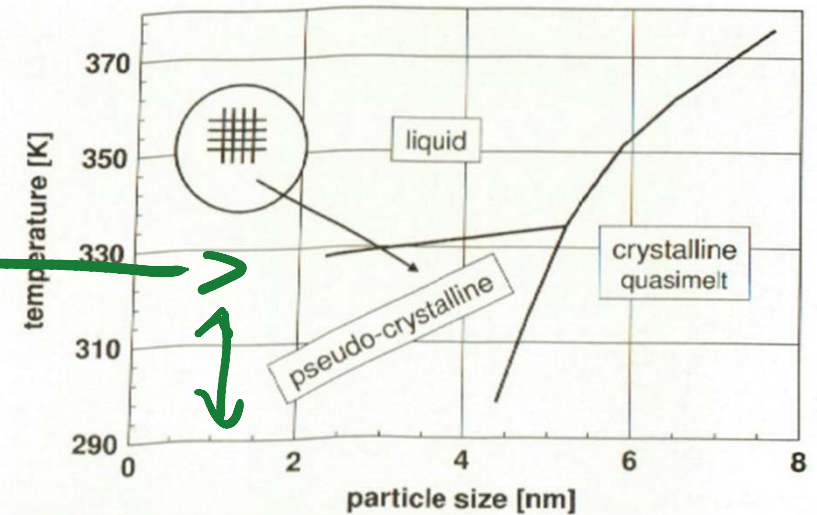


Figure 3.24 Temperature-particle size phase diagram for tin nanoparticles according to Oshima and Takayanagi [21]; conditions as noted for pseudocrystalline particle formation in Figure 3.23 were observed. A schematic drawing of the pseudocrystalline particles is also shown. In the region denominated as crystalline quasimelt, the particles fluctuate between the different possibilities of their habitus.

STRUCTURAL FLUCTUATIONS

kT - MEASURE OF
THERMAL FLUCTUA-
TIONS.

- SUPER PARAMAGNE-
TISM.

$$K_n \cdot \sigma_{nb} \approx kT$$

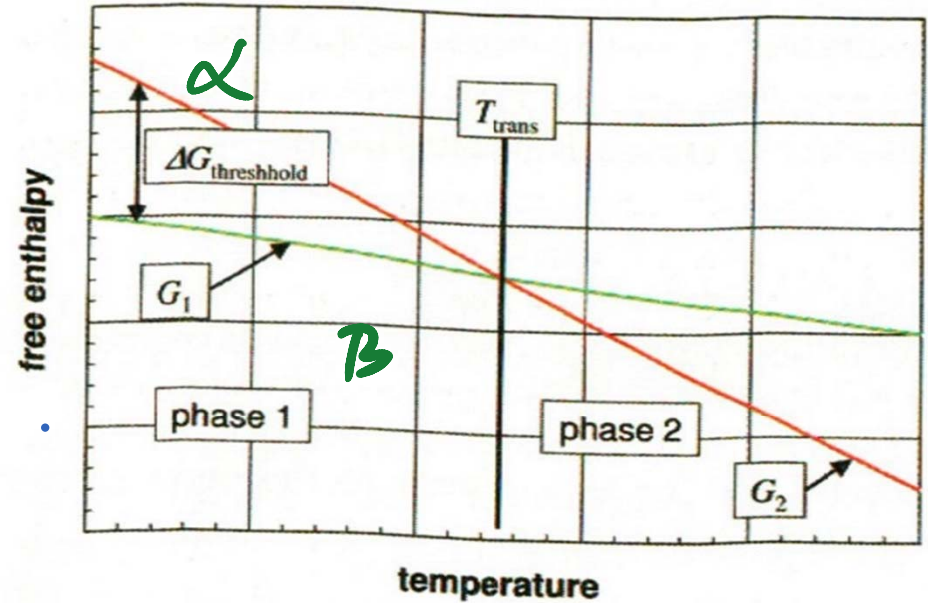


Figure 3.26 Free enthalpy as a function of temperature in the vicinity of a phase transformation. Two areas occur where phases 1 and 2 are stable. However, when $\Delta g_{threshold} < kT$ is fulfilled, spontaneous fluctuations of the individual particles are possible.

STRUCTURAL FLUCTUATIONS

$$\Delta g_{\text{m}} = \Delta G_{\text{m}} \frac{u}{M}$$

$$\Delta g_{\text{m}} \leq kT$$

$$\Delta g_{\text{m}} \sim |T - T_{\text{TRANS}}|$$

$$\Delta g_{\text{m}} = \frac{\delta U_{\text{ms}} \pi D_{\alpha}^3 g_{\alpha}}{6M} - T \Delta S_{\text{ms}} \cdot \frac{\pi D_{\alpha} g_{\alpha}}{6M} + \delta_B \pi D_{\alpha}^2 - \delta_B \pi D_B^2 = kT$$

STRUCTURE FL.

- AFTER RE-ARRANGEMENT.

$$T_R = \frac{\Delta U_{TMS} + \gamma_\alpha \frac{GM}{D_\alpha \rho_\alpha} - \gamma_\beta \frac{GM}{\rho_\beta D_\beta} \left(\frac{\rho_\alpha}{\rho_\beta} \right)^{2/3}}{\Delta S_{TMS} + k \cdot \frac{GM}{\pi D_\alpha^3 \rho_\alpha}}$$

$$T_{FL} \neq T_u$$

$$T_{FL} \sim T_u$$

D → LARGE

D ↓ TERM DOMINATES

D - SMALL

Structure FL.

- TEMPERATURE T_{FL}
- IS VERY DIFFERENT THAN T_m FOR NP.

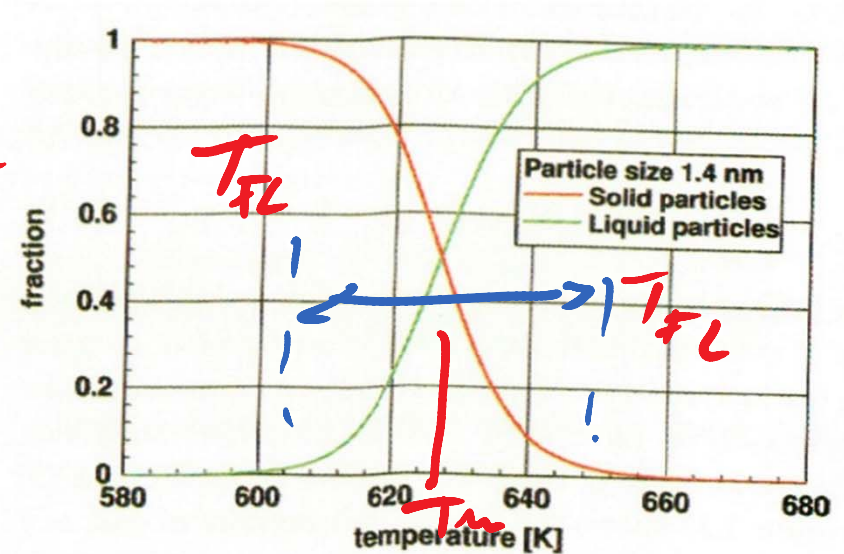


Figure 3.28 Number fractions of gold particles with a diameter of 1.4 nm. Both phases are stable over a broad temperature range [22].

SEE THE MD MOVIES AGAIN!

<https://www.youtube.com/watch?v=MJj5XWQHUFE>

<https://www.youtube.com/watch?v=NWGoE9hwuoo>

https://www.youtube.com/watch?v=AQc_mGjjErAl

